J. Condensed Matter Nucl. Sci. 20 (2016) 54–80

Research Article

Models for the Phase Diagram of Palladium Hydride Including O-site and T-site Occupation

Peter L. Hagelstein*

Massachusetts Institute of Technology, Cambridge, MA, USA

Abstract

Early statistical mechanics models for palladium hydride allowed for a good description of the phase diagram based on a simple parameterization of the O-site energy. In this work we study generalizations of these models to include higher-order dependence on loading, temperature-dependent O-site energies, and also to include T-site occupation. Experimental data sets for 10 isotherms were assembled, and augmented with additional extrapolated points for the low-pressure α-phase region as well as the high pressure β-phase region. Loading-dependent O-site energies are optimized by minimizing the mean square error in the chemical potential between the model and data set. The resulting models give a good match to the phase diagram. If the O-site energy is allowed to be temperature dependent then the fit is better, but the resulting optimum is a mathematical optimum not so closely connected with the physical system. Models were studied in which O-site and T-site occupation occurs. When optimized these models are able to provide a good match to the phase diagram. When the O-site to T-site excitation energy is fixed according to estimates developed in earlier studies, the resulting temperature-dependent O-site energies are physically plausible. When the excitation energy are optimized together with the O-site energy, the resulting optimum is a mathematical one much less connected to the physical system. An earlier analysis of solubility in the α-phase led to a strong argument that T-site occupation occurs in palladium hydride and in palladium deuteriude; the present study supports this conclusion based on an independent data set.
 ISSN 2227-3123

Keywords: Mean field model, Palladium hydride, Phase diagram, Statistical mechanics, T-site occupation

1. Introduction

Palladium hydride [1–5] is perhaps the most studied of the metal hydrides [6–14], in both experiment and theory. Our interest in the problem is motivated by issues associated with the development of models for excess heat in the Fleischmann-Pons experiment [15–17]. In a realistic simulation models are needed for the loading and electrochemical reactions; for hydrogen and deuterium occupation of bulk sites; for vacancy creation and the occupation of vacancy sites. Fundamental to all of these problems are basic statistical mechanics models for hydrogen and deuterium in palladium, which is the focus of the study described in this work. Similar issues arise in the case of modeling nickel systems, which we hope to address in subsequent research.

*E-mail: plh@mit.edu

 ISSN 2227-3123

The first basic statistical mechanics models of this type were described long ago in papers now considered to be classics; by Fowler and Smithells [18]; and by Lacher [19]. Since the chemical potential of hydrogen in gas was known theoretically, it was possible to construct relevant models for hydrogen in palladium since the chemical potentials are equal in equilibrium (the formulations used in the early papers seem more complicated, but are equivalent to matching the solid and gas phase chemical potentials). From a comparison of the model isotherms with data, it was possible to estimate the O-site energy of interstitial hydrogen in Pd, resulting in a statistical mechanics model for part of the phase diagram. In what follows we study generalizations of these models to include higher-order polynomial dependence on loading, temperature-dependent O-site energies, and T-site occupation, to develop models that can describe more of the phase diagram.

To proceed, a set of isotherms are first assembled, and then a set of Lacher models with polynomial dependence of the O-site energy on the loading are optimized. This classic model is found to provide a good match to the data set at elevated temperature, but noticeable deviations occur near room temperature.

In the literature one can find more sophisticated models for interstitial hydrogen in metals termed "lattice gas" models [20–26]. In this case a model Hamiltonian is used with the O-site energy and interactions between the hydrogen atoms specified; statistical mechanics allows for the calculation of the phase diagram or other observables. Model parameters are selected which give the best fit with experiment. The interaction between interstitial hydrogen atoms in the lattice gas model gives rise to a splitting of the energies of the different configurations which cannot be described in terms of a simple loading-dependent O-site energy (independent of temperature). The average O-site energy in this case increases with temperature as more energetic configurations contribute in a statistical mechanics calculation.

Lattice gas models are both interesting and desirable; however, the development and optimization of such models involves significant computation, and research is ongoing to develop models which are better able to match experiment. The focus here is focused on simpler mean field models (alternatively. empirical models) that can be used for applications; our interest in this study is not to determine a better lattice gas Hamiltonian. Nevertheless, we know from these studies, and also from density functional calculations, a substantial splitting of the configuration energies occurs [27,28], and this impacts the empirical models under discussion. In what follows models are considered in which the O-site energy is allowed to depend on temperature, to account approximately for this configurational splitting. The mean-field models when optimized are able to provide better matches to the data set than more basic Lacher models. Unfortunately, the optimized solutions have O-site energies which do not increase with temperature for all loading, and hence are not consistent with a physical model for configurational splitting.

Interstitial hydrogen is known to occupy octahedral sites [29,30], which is consistent with the models discussed so far. In high pressure experiments it is thought that the H/Pd loading has exceeded unity [31,32], conditions under which the occupation of additional sites beyond the O-sites is required. Similar claims have been made for the deuterium loading in electrochemical Fleischmann–Pons experiments [33]. At present the development of over-unity loading of H or D in bulk Pd in any experiment is not universally accepted. There is also not general agreement as to where excess interstitial H or D might go once the O-sites are fully occupied. We have recently studied new models in which both O-site and T-site occupation occurs [34,35], and compared them with experiment in different regimes. Models that include T-site occupation can account for the observed experimental solubility data in the α-phase over a wide range of temperatures [34], conditions where models with only O-site occupation have trouble. Estimates for the O-site to T-site excitation energy for α-phase PdH_x and PdD_x near 100 meV resulted from this study. The new models were used to compare with experiment in the β-phase [35] and higher, which resulted in a parameterization of the loading-dependent O-site to T-site excitation energy near room temperature.

As indicated above the primary motivation for this work is to develop simple mean-field models that can be used for applications. However, another motivation was to see whether models developed for O-site to T-site occupation were compatible with the isotherms of the phase diagram. A related issue is whether T-site occupation is necessary to understand the phase diagram. We know from previous work that T-site occupation is required to model loading

in the α-phase; however, whether T-site occupation is needed for the rest of the phase diagram has not previously been addressed. In the end, our results suggest that it may not be possible to develop an accurate model that is also acceptable on physical grounds without T-site occupation.

2. Isotherms and Phase Diagram

The first task is to assemble isotherms for a reference phase diagram. Since palladium hydride is perhaps the best studied of the metal hydrides, there are many data sets with which to work. We made use of a subset of isotherms presented by Manchester et al. [4], which recommended itself since a sizeable collection of individual pressure-composition-temperature (PCT) data points were plotted. The online web digitization program of Ankit Rohagti allowed for the conversion of the published data points into digital form.

It was found necessary to extend the isotherms to lower loading in the α-phase, and also to higher loading in the β-phase. Reliable isotherms for the α-phase could be constructed based on an empirical fit to literature data as described in the following subsection. For high concentration a (less reliable) generalization of an empirical fit due to Baranowski et al. [31] was used. This allowed for a "complete" set of isotherms at ten different temperatures between 20°C and 433°C which could be used for fitting statistical mechanics model parameters.

Extrapolated α-phase data points at low pressure are needed to provide an "anchor" for the model at low loading. There is a differential relation between the O-site and T-site energies, and the chemical potential; consequently, a boundary condition is required in order to determine a unique solution for the chemical potential as a function of loading. The extrapolated low pressure points serve to fix the boundary condition in the optimizations. Good agreement using this approach is found with the results obtained previously based on a different data set (the data set of Clewley et al. [36]).

The biggest issue with the extrapolated points at high loading is that far fewer experimental studies have been published, so that the development of an accurate extrapolation is problematic. Another concern is that if T-site occupation is significant, then there is reason to be concerned whether the extrapolation used includes it (and there is no reason to believe it does). Consequently, it would not be expected that a reliable O-site to T-site excitation energy can be determined at high loading from the isotherms, since the impact of T-site occupation is greatest at high temperature where there is no data at high loading.

2.1. Empirical fit for the α-phase

Empirical fits for the α-phase have been studied previously [18,37–43]; for example Simons and Flanagan [39] give the empirical formula (in our notation)

$$\ln P(\mathrm{atm}) = 13.04 - \frac{2327}{T} - \frac{11110}{T}\theta + 2\ln\frac{\theta}{1-\theta}. \tag{1}$$

It was found that this formula is useful over a restricted temperature range. A new empirical formula was developed based on

$$\ln P(\mathrm{atm}) = \left(\frac{a_{-1}}{T} + a_0 + a_1 T\right) + \left(\frac{b_{-1}}{T} + b_0 + b_1 T\right)\theta + 2\ln\frac{\theta}{1-\theta}. \tag{2}$$

The fitting parameters were optimized to give

$$a_{-1} = -2478.35\,\mathrm{K}, \quad a_0 = 14.1429, \quad a_1 = -0.00204315\,\mathrm{K}^{-1},$$

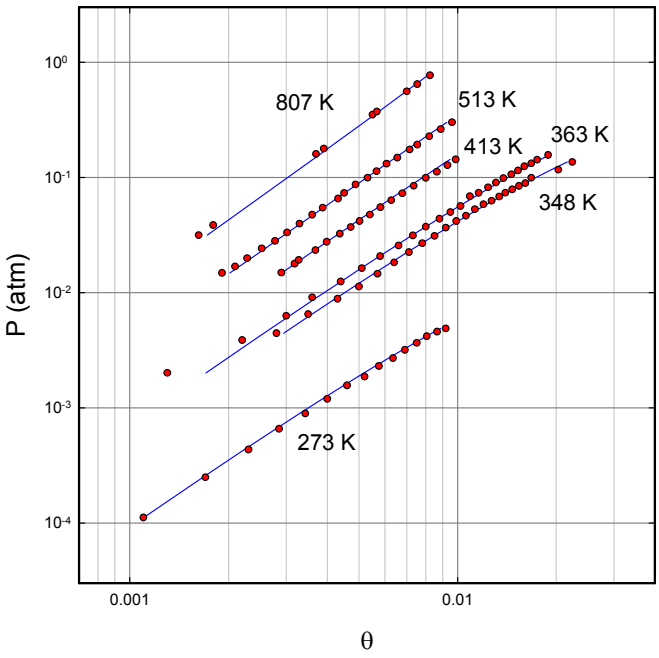

Figure 1. Solubility data in the α-phase region of PdH_x (*red triangles*); empirical fit (*blue lines*).

$$b_{-1} = -24147.1\,\mathrm{K}, \quad b_0 = 57.5628, \quad b_1 = -0.0534775\,\mathrm{K}^{-1}. \tag{3}$$

The resulting empirical fit is compared with data used for parameter optimization in Fig. 1. For the data sets at 273, 348 and 363 K we used the tabulated data of Simons and Flanagan [39]; the isotherms at 413 and at 513 K are from Oates et al. [44]; and the solubility data at 807 K is from Kleppa and Phutella [42].

2.2. Empirical fit at high loading

At high loading there are empirical formulas in the literature, such as the empirical fit of Baranowski et al. [31] given by

$$\ln f_{H_2} = \frac{-(100.4 - 90.1\theta)(\mathrm{kJ/mol})}{RT} + \frac{106.4\mathrm{J/(mol\,K)}}{R} + 2\ln\frac{\theta}{1-\theta}. \tag{4}$$

Motivated by this, we decided to construct an empirical fit of the form

$$\ln f_{H_2} = \frac{(a_0 + b_0\theta)}{T} + \Big(a_1 + b_1\theta\Big) + T\Big(a_2 + b_2\theta\Big) + 2\ln\frac{\theta}{1-\theta} + 2\frac{PV_H}{k_B T}. \tag{5}$$

This fit includes the next order in temperature, and adds a $P\,\mathrm{d}V$ term. The fitting parameters are:

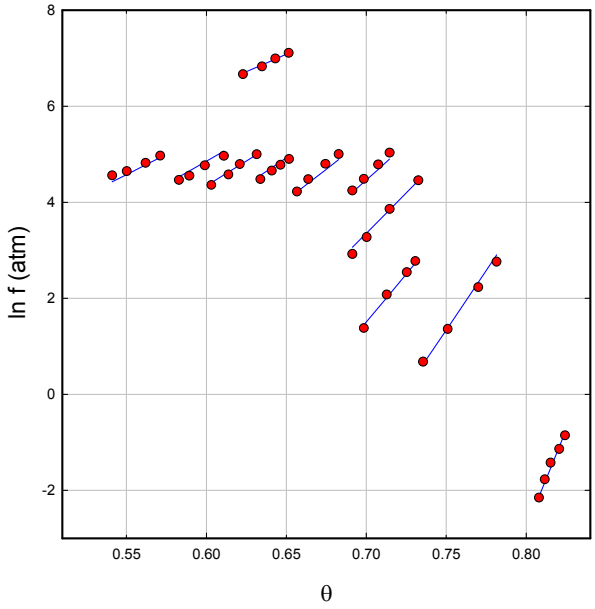

Figure 2. Data points and fit for the empirical model at high pressure.

$$a_0 = -18215.5\,\mathrm{K}, \quad b_0 = 17469.8\,\mathrm{K}, \quad a_1 = 35.3611, \quad b_1 = -22.1764,$$

$$a_2 = -0.0102061\,\mathrm{K}^{-1}, \quad b_2 = 0.0038497\,\mathrm{K}^{-1} \tag{6}$$

with fugacity in atmospheres. This empirical fit is compared against the high loading data points from our data set in Fig. 2.

2.3. Isotherms

The resulting isotherms are shown in Fig. 3. We selected data sets from Manchester et al. [4] for 20, 70, 120, 160, 200, 243, 270, 300, 340, and 433°C; and we extended the data set to both lower and higher H/Pd loadings using the extrapolations described in this section.

3. Model with Loading-dependent O-site Energy

The first realistic model for the phase diagram of PdH was put forth in Lacher's classic paper [19], which assumed that the O-site energy is quadratic in the loading and independent of temperature. Models of this kind have been used to predict phase diagrams previously [19,45,46]. In this section O-site energy models that are polynomial in loading are optimized against the reference isotherm data set to determine fitting parameters.

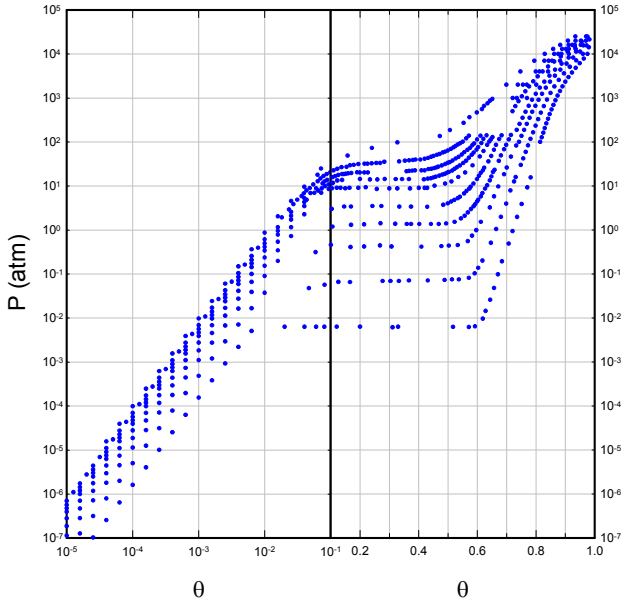

Figure 3. Data points used in this study for the isotherms of the phase diagram.

3.1. Model

A model for O-site occupation can be derived by assuming that hydrogen is in equilibrium in the gas phase and solid phase, so that the chemical potential in the two phases match

$$\mu_{\rm H}^{\rm s} = \mu_{\rm H}^{\rm g} = \frac{1}{2}\mu_{\rm H_2}^{\rm g}. \tag{7}$$

The chemical potential in the gas phase is accurately known. For the solid phase and only O-site occupation we may write [34]

$$\mu_{\rm H} = E_{\rm O} + \theta\frac{\partial E_{\rm O}}{\partial\theta} - k_{\rm B}T\ln\frac{1-\theta}{\theta} - k_{\rm B}T\ln z_{\rm O} + PV_{\rm H}, \tag{8}$$

where $E_{\rm O}$ is the O-site energy which depends on the loading θ, and may also depend on temperature in some of the models under consideration.

3.2. O-site partition function

For the modeling in this work a non-SHO O-site partition function is used as discussed in [34]. For O-site occupation the partition function is taken to be

$$z_{\rm O} = 4\left(\sum_n \exp\left\{-\frac{E_n}{k_{\rm B}T}\right\}\right)^3 \tag{9}$$

with

$$E_n = \hbar\omega_{\rm O} n^{\rm s}. \tag{10}$$

The excitation energy and scaling parameter for O-site occupation are

$$\hbar\omega_{\rm O} = 69.0\ {\rm meV}, \quad s_{\rm O} = 1.2. \tag{11}$$

3.3. Optimization

For the optimization in this work, a measure of the error I is defined according to

$$I = \frac{1}{N}\sum_j \left[\mu_{\rm H}({\rm data}) - \mu_{\rm H}({\rm model})\right]_j^2, \tag{12}$$

where the summation is over all of the data points of the isotherms in the phase diagram. The hydrogen in gas chemical potential [34,35] is determined at the loading of a given data point, and then compared with the chemical potential for the hydrogen in solid determined from the model under consideration. The model parameters are optimized from a minimization of the resulting mean square error I.

3.4. O-site energy results

We optimized models with polynomial O-site energy of the form

$$E_{\rm O}(\theta) = a_0 + a_1\theta + a_2\theta^2 + a_3\theta^3 + a_4\theta^4 + a_5\theta^5 + a_6\theta^6 \tag{13}$$

for polynomial O-site energy models models with third- to sixth-order dependence on the loading θ. The errors associated with the different optimizations are given in Table 1. One sees that the errors are smaller for higher-order models.

Table 1. Error associated with the optimization of the different models assuming θ-dependent O-site energies considered in this section.

Order	I
3	4.22×10^{-4}
4	1.63×10^{-4}
5	1.37×10^{-4}
6	1.34×10^{-4}

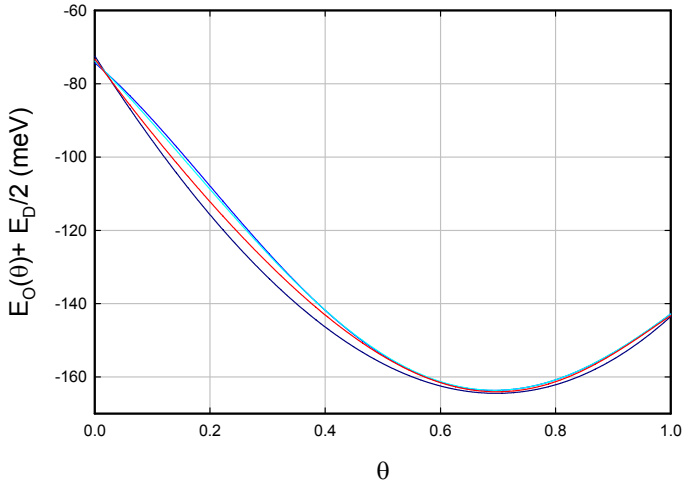

Figure 4. O-site energy as a function of θ with only O-site occupation; third-order polynomial (*dark blue line*); fourth-order polynomial (*blue line*); fifth-order polynomial (*cyan line*); and sixth-order polynomial (*red line*).

Results for the O-site energy are shown in Fig. 4. There are minor differences in the different models, with a general convergence toward a curve close to the sixth-order polynomial model result. Fitting parameters for the sixth-order optimized O-site energy are given by

$$a_0 = -73.244, \quad a_1 = -211.382, \quad a_2 = 67.137, \quad a_3 = 93.793$$

$$a_4 = -212.541, \quad a_5 = 404.335, \quad a_6 = -211.373 \tag{14}$$

with individual a_j coefficients in meV.

3.5. Comparison of predicted phase diagram with experiment

The phase diagram for the sixt-order polynomial fit for $E_{\rm O}$ is shown in Fig. 5. In general this model does pretty well; however, the predicted isotherms lie noticeably above the experimental data points at the lower temperatures.

4. O-site Energy Dependent on Loading and Temperature

In a more sophisticated lattice gas treatment the different configurations (corresponding to different arrangements of hydrogen atoms in different lattice sites) have different energies. Consequently, the use of a loading-dependent O-site energy itself constitutes a significant approximation (in the literature this is referred to as a mean-field approximation). Here we make use of a mean field approximation where the (mean) O-site energy is allowed to depend both on loading and on temperature. As before the fitting parameters of the O-site energy are determined by optimization against the reference phase diagram.

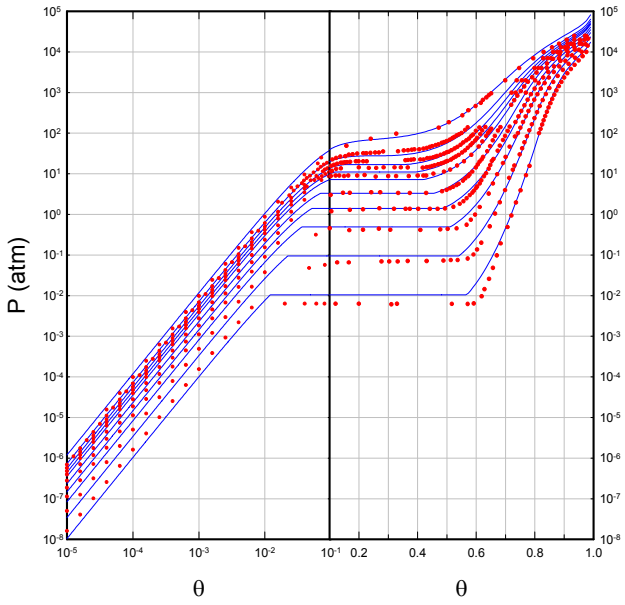

Figure 5. Isotherms and data points for the temperature-independent sixth-order polynomial fit of $E_{\rm O}$.

Some intuition about how this model might work seems useful here. If there is a substantial splitting in the different configuration energies, we would expect this to be captured in the empirical model with model O-site energies lower at low temperature, and model O-site energies higher at high temperature. This will provide a check on the results, to make sure that the intended physics is captured in the optimization results.

4.1. Model and optimization

We have optimized models with a polynomial dependence on loading as before, but now the model is expanded to assume in addition a linear dependence on the temperature according to

$$E_{\rm O}(\theta,T) = \left[a_0 + a_1\theta + a_2\theta^2 + a_3\theta^3 + a_4\theta^4 + a_5\theta^5 + a_6\theta^6\right] + T\left[b_0 + b_1\theta + b_2\theta^2 + b_3\theta^3 + b_4\theta^4 + b_5\theta^5 + b_6\theta^6\right]. \quad (15)$$

We have optimized the model parameters by minimizing the associated error I as described in the previous section. The additional degrees of freedom have allowed for the error I to be significantly reduced, as can be seen by comparing the results of Table 1 with those of Table 2.

Table 2. Errors associated with the optimization of the different models with O-site occupation considered in this section.

a,b order	I
3,3	1.67×10^{-4}
4,4	4.40×10^{-5}
5,5	2.06×10^{-5}
6,6	2.01×10^{-5}

4.2. O-site energies

The optimized O-site energies that result for the model with sixth-order polynomial dependence on the loading is shown in Fig. 6. The associated expansion coefficients are

$$a_0 = -57.269, \quad a_1 = -269.674, \quad a_2 = 42.263, \quad a_3 = -10.436,$$

$$a_4 = 376.561, \quad a_5 = -222.779, \quad a_6 = -7.575,$$

$$b_0 = -0.0282103, \quad b_1 = 0.1068191, \quad b_2 = 0.3125901, \quad b_3 = -1.0341667,$$

$$b_4 = 1.0675563, \quad b_5 = -0.4938008, \quad b_6 = 0.0728168. \tag{16}$$

The a_j coefficients are in meV, and the b_j coefficients are in meV/K.

We see a modest spread in the O-site energies, with the O-site energy increasing with temperature at high loading (as would be expected for a physical system). At low loading, the O-site energy appears to decrease with temperature,

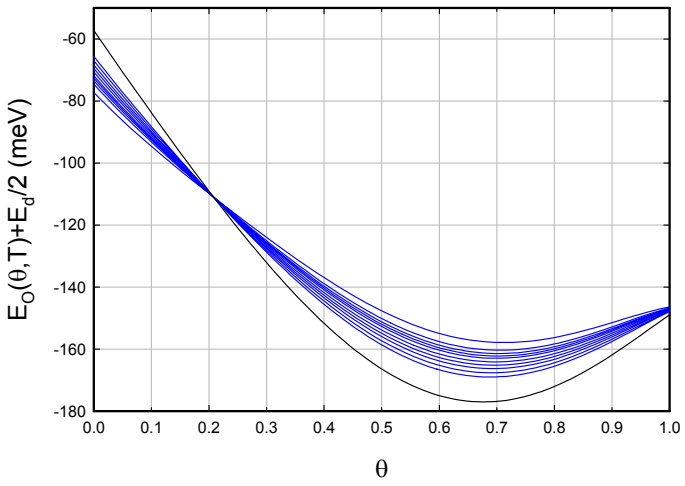

Figure 6. O-site energies as a function of loading for the different temperatures of the isotherms (*blue lines*); extrapolation to $T = 0$ (*black line*).

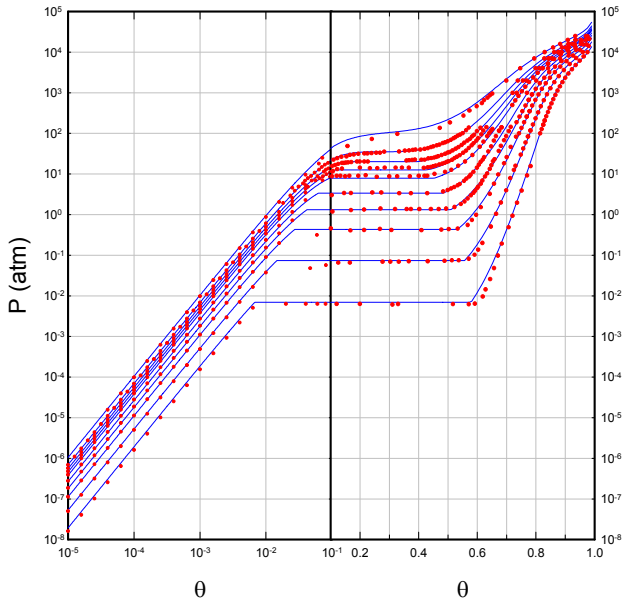

Figure 7. Isotherms and data points for the temperature-dependent sixth-order polynomial fit of $E_{\rm O}$.

an effect not consistent with our picture above involving a spread in O-site energies. Consequently, we recognize that this optimized model corresponds to a mathematical optimum, but one that is not particularly closely connected to a physical picture at low loading.

4.3. Model phase diagram

Given the reduced error associated with the optimization of the models, the fit to the isotherms is expected to be improved. This can be seen in the associated phase diagram for the lowest error sixth-order polynomial model in Fig. 7. The agreement is now better for the lower temperature isotherms.

5. Inclusion of T-site Occupation with a Model Excitation Energy

As discussed briefly in the Introduction the issue of T-site occupation in palladium hydride is controversial; based on the results of modern density functional calculations T-site occupation should be expected, but there is not at present an unambiguous experimental demonstration of T-site occupation. In previous work we made estimates for the O-site to T-site excitation in the α-phase [34] and in the β-phase [35]. In this section we make use of these earlier estimates for the excitation energy to construct a statistical mechanics model that can be fit to experimental data. The O-site to T-site excitation energy in this case is assumed to depend on loading, but not on temperature.

5.1. Model for O-site and T-site occupation

A model for the chemical potential in terms of the O-site and T-site loading $\theta_{\rm O}$ and $\theta_{\rm T}$, in terms of the O-site and T-site energies $E_{\rm O}$ and $E_{\rm T}$, was developed previously [35]. The chemical potential for interstitial hydrogen in O-sites and in T-sites is given by

$$\mu_{\rm H} = E_{\rm O} + \theta_{\rm O}\frac{\partial E_{\rm O}}{\partial\theta} + \theta_{\rm T}\frac{\partial E_{\rm T}}{\partial\theta} - k_{\rm B}T\ln\frac{1-\theta_{\rm O}}{\theta_{\rm O}} - k_{\rm B}T\ln z_{\rm O}, \tag{17}$$

$$\mu_{\rm H} = E_{\rm T} + \theta_{\rm T}\frac{\partial E_{\rm T}}{\partial\theta} + \theta_{\rm O}\frac{\partial E_{\rm O}}{\partial\theta} - k_{\rm B}T\ln\frac{2-\theta_{\rm T}}{\theta_{\rm T}} - k_{\rm B}T\ln z_{\rm T}. \tag{18}$$

Subtracting these two relations leads to

$$E_{\rm T} - E_{\rm O} = k_{\rm B}T\left\{\ln\left(\frac{2-\theta_{\rm T}}{\theta_{\rm T}}\frac{\theta_{\rm O}}{1-\theta_{\rm O}}\right) + \ln\frac{z_{\rm T}}{z_{\rm O}}\right\}. \tag{19}$$

This we solve to determine $\theta_{\rm T}$ given $\theta_{\rm O}$, and then make use of Eq. (17) for the chemical potential of H in the solid phase.

5.2. T-site partition function

In this analysis we have made use of a non-SHO T-site partition function of the form

$$z_{\rm T} = 4\left(\sum_n \exp\left\{-\frac{E_n}{k_{\rm B}T}\right\}\right)^3 \tag{20}$$

with

$$E_n = \hbar\omega_{\rm T} n^{\rm s}. \tag{21}$$

The excitation energy and scaling parameter for O-site occupation are

$$\hbar\omega_{\rm T} = 53.8\ {\rm meV}, \quad s_{\rm T} = 1.2. \tag{22}$$

5.3. O-site to T-site excitation energy

For T-site occupation we make use of a model for the O-site to T-site energy parameterized by

$$\Delta E(\theta) = \frac{\alpha_0 + \alpha_1\theta}{1+\beta_1\theta} + 1\ {\rm meV} \tag{23}$$

with fitting parameters

$$\alpha_0 = 100.676\ {\rm meV}, \quad \alpha_1 = 824.259\ {\rm meV\ K^{-1}}, \quad \beta_1 = 3.1108\ {\rm K^{-1}}. \tag{24}$$

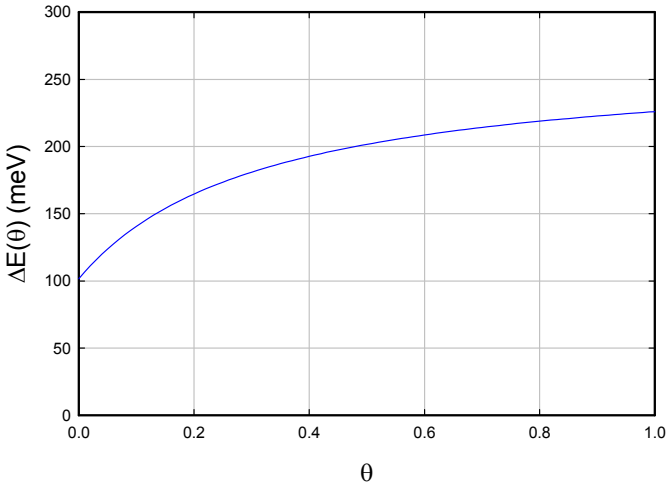

Figure 8. Empirical model for the O-site to T-site excitation energy as a function of loading θ.

This empirical model is shown in Fig. 8. Estimates for the excitation energy in the α-phase near $\theta = 0$ and in the β-phase near $\theta = 1$ were developed previously from the analyses reported in [34,35]. For the intermediate loading regime the neutron diffraction measurements of Pitt and Gray [47] can be interpreted in terms of an excitation energy for palladium deuteride. Based on our earlier analysis we would expect that the O-site excitation energy is probably similar for palladium hydride near room temperature and above.

5.4. Models based on a temperature-independent O-site energies

We have optimized a set of models with O-site and T-site occupation assuming a temperature-independent O-site energy model. The errors are given in Table 3.

The fitting coefficients (in meV) for the sixth-order polynomial solutions are

$$a_0 = -62.763, \quad a_1 = -249.626, \quad a_2 = 173.686, \quad a_3 = -91.330,$$

$$a_4 = 32.832, \quad a_6 = -110.942. \tag{25}$$

Table 3. Errors associated with the optimization of models with O-site and T-site occupation considered in this subsection.

Order	I
3 | ΔE model	4.22×10^{-4}
4 | ΔE model	4.19×10^{-4}
5 | ΔE model	4.09×10^{-4}
6 | ΔE model	4.05×10^{-4}

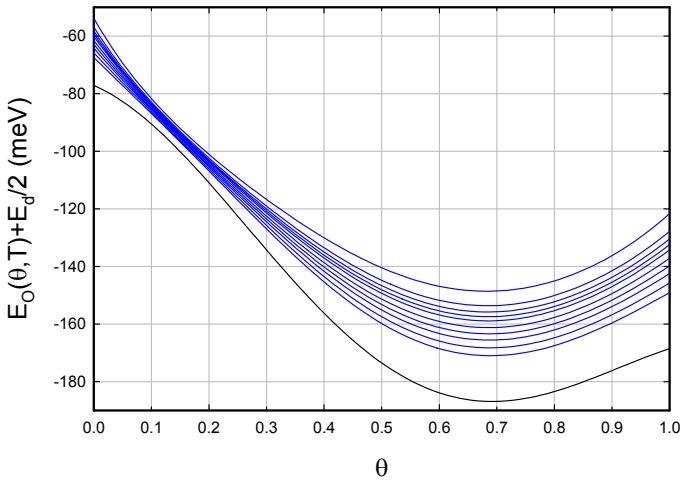

Figure 9. O-site energies as a function of loading for the different temperatures of the isotherms (*blue lines*); extrapolation to $T = 0$ (*black line*).

In this case lower errors would have been obtained with no T-site occupation, as we can see by comparing with Table 1. According to this there is no benefit (in terms of error reduction) to augmenting a model based on O-site occupation with a temperature-independent $E_{\rm O}(\theta)$ so that it includes T-site occupation based on the $\Delta E(\theta)$ model given above.

5.5. Temperature-dependent O-site energy

Next we consider models based on an O-site energy that depends on both loading and on temperature, combined with a T-site model based on the O-site to T-site excitation energy given above. The intention here is to account for the configurational splitting discussed above, and by doing so reduce the associated optimization error. Results for the errors are given in Table 4.

Results for the different O-site energies for the sixth-order version of the model are shown in Fig. 9. In contrast to the previous unphysical results for the temperature-dependent O-site energies in the last section (Fig. 6), these O-site energies are increasing with increasing temperature. Also, the increase in the O-site energy at $\theta = 0$ is now comparable to what was found in our earlier analysis of the α-phase solubility in Ref. [34].

The fitting coefficients for the 6th-order polynomial model are

Table 4. Errors associated with the optimization of the different models with O-site and T-site occupation considered in this section.

a,b Order	I
3,3 | ΔE model	8.07×10^{-5}
4,4 | ΔE model	2.99×10^{-5}
5,5 | ΔE model	2.65×10^{-5}
6,6 | ΔE model	1.93×10^{-5}

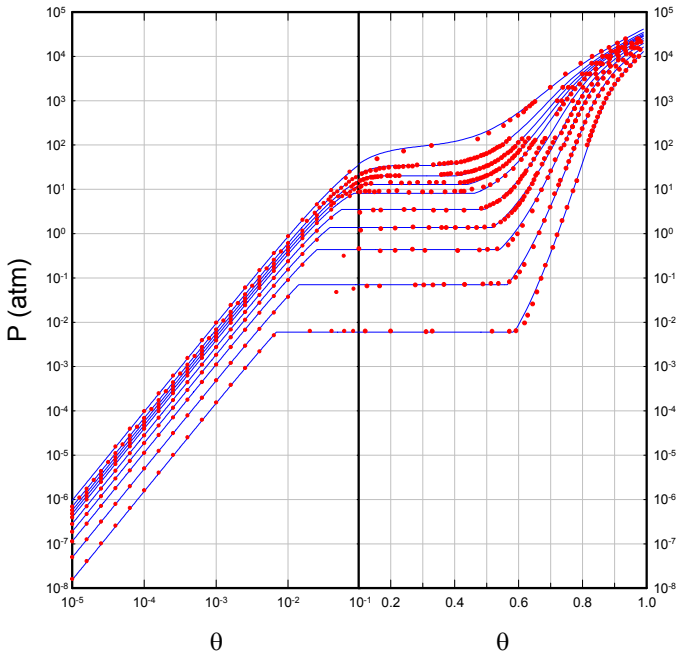

Figure 10. Isotherms and data points for the model with temperature-dependent 6th-order polynomial fit of $E_{\rm O}$ and an empirical ΔE model.

$$a_0 = -77.093, \quad a_1 = -92.584, \quad a_2 = -496.658, \quad a_3 = 361.628,$$

$$a_4 = 940.828, \quad a_5 = -1130.451, \quad a_6 = 325.675,$$

$$b_0 = 0.0330887, \quad b_1 = -0.3739481, \quad b_2 = 2.0569084, \quad b_3 = -3.9515725,$$

$$b_4 = 3.7471947, \quad b_5 = -1.9623168, \quad b_6 = 0.5147468, \tag{26}$$

where the a_j coefficients are in meV, and the b_j coefficients are in meV/K.

5.6. Phase diagram

The phase diagram that results is shown in Fig. 10. Although there are minor issues, in general this appears to be a pretty solid match between model and data. We have in this model succeeded in obtaining a good match with the phase diagram with a model that is physically plausible.

6. Unconstrained Models with Both O-site and T-site Occupation

In the previous section we made use of a fixed model for O-site to T-site excitation energy based on earlier analyses with different data sets. In this section we allow for the loading-dependent excitation energy itself to be determined directly as a result of the optimization. The motivation for this is to see whether the phase diagram data set itself can be used to provide an independent estimate for the O-site to T-site excitation energy.

6.1. Models with temperature-dependent O-site energy

We discussed above that there is a spread in the energies of the different configurations for partially loaded palladium hydride, and that a crude way to account for this might be to work with a temperature-dependent O-site energy. The O-site energy in this case is parameterized using fifth-order polynomials in loading according to

$$E_{\rm O}(\theta,T) = \left[a_0 + a_1\theta + a_2\theta^2 + a_3\theta^3 + a_4\theta^4 + a_5\theta^5\right] + T\left[b_0 + b_1\theta + b_2\theta^2 + b_3\theta^3 + b_4\theta^4 + b_5\theta^5\right]. \quad (27)$$

The O-site to T-site excitation energy is similarly parameterized according to

$$\Delta E(\theta) = d_0 + d_1\theta + d_2\theta^2 + d_3\theta^3 + d_4\theta^4 + d_5\theta^5. \quad (28)$$

We have optimized a set of models of this kind, with the results of optimization listed in Table 5. We see that the associated errors are lower than what we found for all other models considered in this work.

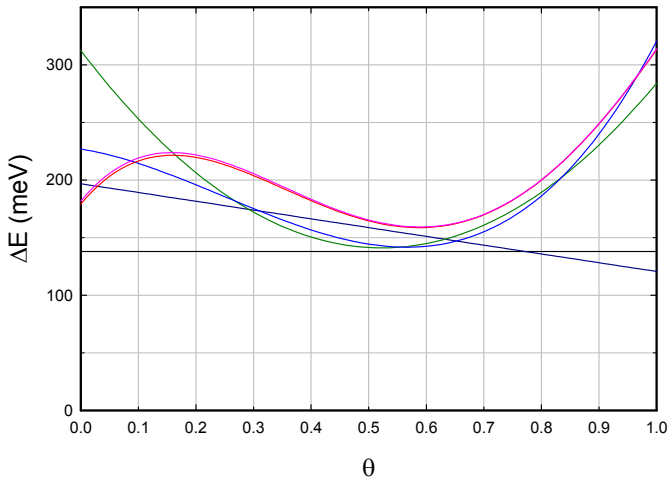

Figure 11. O-site to T-site excitation energy as a function of θ, for models with temperature-dependent O-site energy $E_{\rm O}$ and unconstrained temperature-independent O-site to T-site excitation energy; ΔE linear in θ (*dark blue line*); second-order model (*dark green line*); third-order model (*blue line*); fourth-order model (*red line*); fifth-order model (*pink line*).

The fitting coefficients for the lowest error fifth-order polynomial solution are:

$$a_0 = -65.426, \quad a_1 = -5.627, \quad a_2 = -1099.972,$$

$$a_3 = 1503.386, \quad a_4 = -266.445, \quad a_5 = -226.248,$$

$$b_0 = -0.007048, \quad b_1 = -0.364993, \quad b_2 = 2.052026,$$

$$b_3 = -2.207565, \quad b_4 = -0.033973, \quad b_5 = 0.596698,$$

$$d_0 = 178.523, \quad d_1 = 615.281, \quad d_2 = -2641.792,$$

$$d_3 = 3242.712, \quad d_4 = -1066.321, \quad d_5 = -17.063, \tag{29}$$

where the a_j and d_j coefficients are in meV, and the b_j coefficients are in meV/K.

6.2. O-site to T-site excitation energy

These results support the notion that T-site occupation occurs in palladium hydride, since we obtain better agreement with the phase diagram when T-site occupation is included. The optimized O-site to T-site excitation energies (shown in Fig. 11) are between about 100 and 300 meV, which are in the general range of what we estimated in earlier studies [34,35]. We note that the fifth-order polynomial curve with the lowest associated error lies well above the empirical model of Fig. 8 at $\theta = 0$, where we have some confidence in the excitation energy based on our analysis of the α-phase experimental data. It also lies well above the empirical model of Fig. 8 where we have some confidence in the analysis of experimental results at high loading.

6.3. O-site energy

Next consider the spread of O-site energies for the lowest error model, shown in Fig. 12. We recall that in the physical system there is a spread in the energies of the different configuration, which we seek to model with a temperature-dependent O-site energy. At high loading the O-site energies are seen to increase with temperature, consistent with the splitting effect under consideration. However, at low loading the situation is reversed. We recognize this solution as a mathematical optimum, and not as an acceptable physical solution.

Table 5. Errors associated with the unconstrained optimization of different models with O-site and T-site occupation.

a,b | d order	I
5,5 | 0	2.17×10^{-5}
5,5 | 1	2.03×10^{-5}
5,5 | 2	1.34×10^{-5}
5,5 | 3	9.28×10^{-6}
5,5 | 4	8.22×10^{-6}
5,5 | 5	8.08×10^{-6}

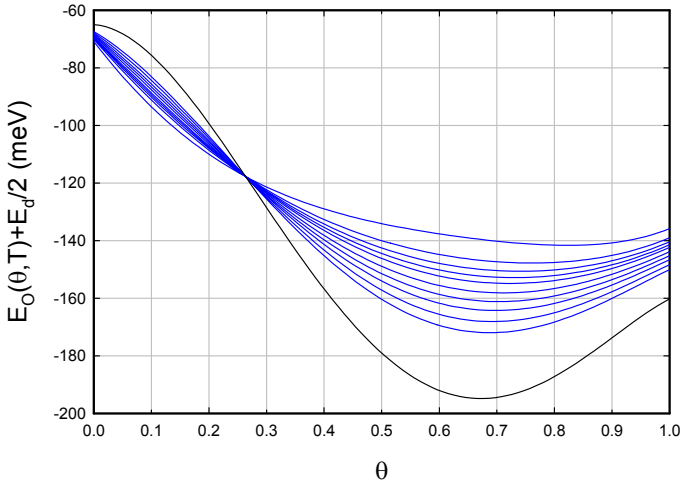

Figure 12. O-site energies as a function of loading for the different temperatures of the isotherms (*blue lines*); extrapolation to $T = 0$ (*black line*). Above an H/Pd loading of 0.26 the curves are ordered with increasing excitation energy corresponding to increasing temperature.

6.4. Phase diagram

The phase diagram for the model with the lowest error is shown in Fig. 13. The fit is very good, as expected.

7. Constrained Models with Both O-site and T-site Occupation

The low errors found in the optimization of the previous section provide motivation to consider a constrained optimization, where the O-site to T-site excitation energy is again determined based on optimization, but now we constrain the excitation energy to values estimated in previous work at $\theta = 0$ and at $\theta = 1$. It is possible that an independent estimate for the excitation energy at intermediate loading can be determined from this kind of optimization.

7.1. Model

In this case we use an excitation energy of the form

$$\Delta E(\theta) = d_0 + d_1\theta + d_2\theta^2 + d_3\theta^3 + d_4\theta^4 + d_5\theta^5$$

with [34]

$$d_0 = 101.676\,\mathrm{meV}. \tag{30}$$

For the O-site energy, we made use of fifth-order polynomials in θ and assumed a linear temperature dependence as before.

The optimization is carried out on the modified error J given by

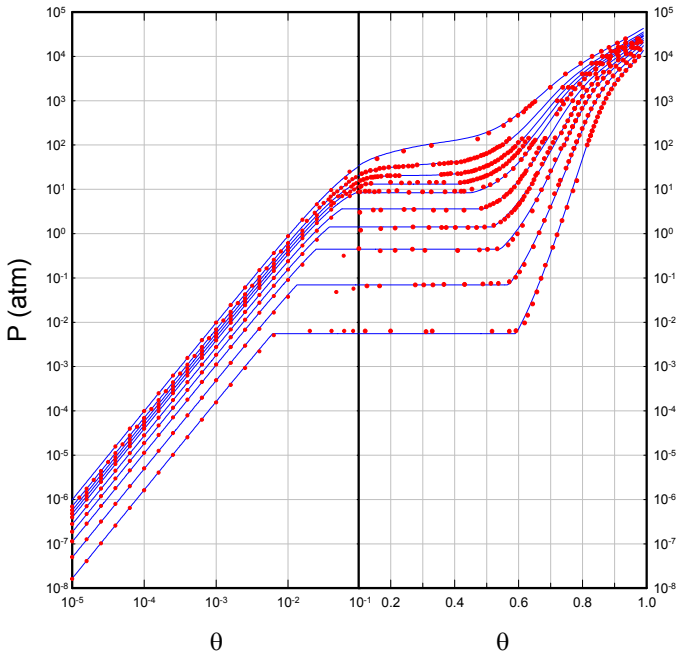

Figure 13. Isotherms and data points for the model with temperature-dependent fifth-order polynomial fit of $E_{\rm O}$ and optimized fifth-order model for $\Delta E(\theta)$.

$$J = \frac{1}{N}\sum_j \left[\mu_{\rm H}({\rm data}) - \mu_{\rm H}({\rm model})\right]_j^2 + \gamma\left(226\ {\rm meV}\ - \sum_{i=0}^{5} d_i\right)^2. \tag{31}$$

We choose low values for γ in the vicinity of unity for the initial optimizations, and then later on increase γ to 100. This leads to values of ΔE at $\theta = 1$ close to 226 meV.

7.2. Results

Constrained optimizations have been carried out on a set of models with the results given in Table 6. The errors I (see Eq. (12)) that result are larger than what we obtained in the unconstrained optimizations of the previous section (see Table 5). There is a minor penalty associated with imposing constraints on the model parameters.

The fitting coefficients for the lowest error model with fifth-order polynomial fits are

$$a_0 = -77.889, \quad a_1 = -6.933, \quad a_2 = -1102.321,$$

$$a_3 = 1616.798, \quad a_4 = -453.666, \quad a_5 = -149.614,$$

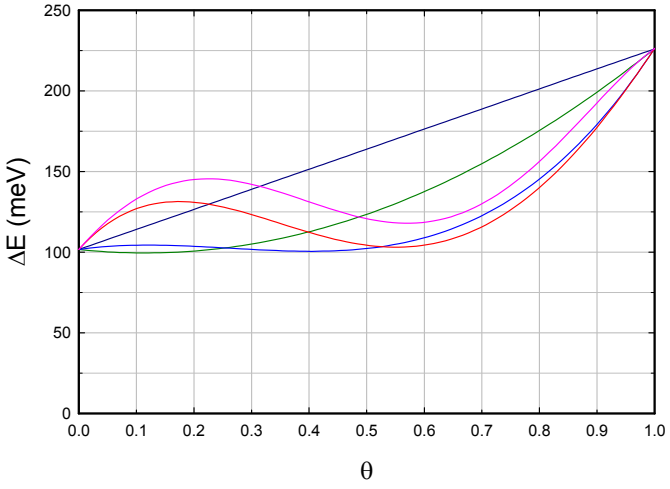

Figure 14. O-site to T-site excitation energy as a function of θ, for models with temperature-dependent O-site energy $E_{\rm O}$ and temperature-independent O-site to T-site excitation energy; ΔE linear in θ (*dark blue* line); second-order model (*dark green* line); third-order model (*blue line*); fourth-order model (*red line*); fifth-order model (*pink line*).

$$b_0 = 0.034584, \quad b_1 = -0.454285, \quad b_2 = 2.306099,$$

$$b_3 = -2.428471, \quad b_4 = -0.179903, \quad b_5 = 0.805586,$$

$$d_1 = 413.703, \quad d_2 = -951.745, \quad d_3 = -612.564,$$

$$d_4 = 2793.066, \quad d_5 = -1517.832, \tag{32}$$

where the a_j and d_j are in meV, and the b_j are in meV/K.

7.3. Excitation energy

The excitation energy for the different versions of the model are shown in Fig. 14. The models converge slowly with order (and have not finished converging as a function of the polynomial order), with the O-site to T-site excitation

Table 6. Errors associated with the constrained optimization of the different models with O-site and T-site occupation considered in this section.

a,b | d Order	I
5,5 | 1	2.71×10^{-5}
5,5 | 2	2.47×10^{-5}
5,5 | 3	2.16×10^{-5}
5,5 | 4	1.70×10^{-5}
5,5 | 5	1.50×10^{-5}

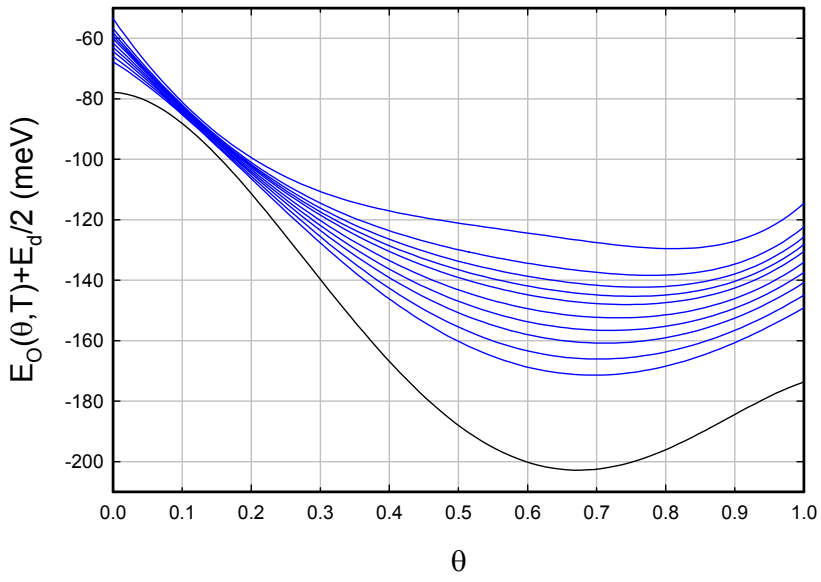

Figure 15. O-site energies as a function of loading for the different temperatures of the isotherms (*blue lines*); extrapolation to $T = 0$ (*black line*).

energy for the fifth-order model (*in pink*) first increasing with loading, then decreasing, and then increasing again. This reversal leads to low values for the excitation energy going down to about 117 meV at $\theta = 0.56$. This reversal moves the excitation energy sufficiently low to be in disagreement with the neutron diffraction data for palladium deuteride.

7.4. O-site energy

The O-site energies for the lowest error version of the model are shown in Fig. 15. Constraining the excitation energy at $\theta = 0$ results in O-site energies which seem generally reasonable. We might also expect the largest change with temperature to occur generally in the vicinity of $\theta = 1/2$, since this is where the splitting is probably largest. We see in Fig. 15 that the largest increase in temperature occurs at a loading closer to $\theta = 0.66$, and that there is a decrease for larger θ. Such a behavior might be explained if there is an additional thermal effect, such as an increase in lattice expansion with temperature at high loading.

The spread in O-site energy for these models has gotten sufficiently large in this case that we would be concerned about the resulting model being acceptable on physical grounds. If the excitation energy were larger in the general vicinity of $\theta = 1/2$, then the spread would be reduced. This suggests that an excitation energy more consistent with the neutron diffraction experiments in this regime would result in a more physical and better model.

There is a spread near $\theta = 0$ which is worth some discussion. We note that we found a similar increase in the O-site energy with temperature in our previous analysis of solubility for α-phase PdH_x and PdD_x [34]. There is agreement in the magnitude of this effect in the different models (of this work, and of the previous one), which are derived from different data sets; this is encouraging, and suggests consistency both in the experimental data and in the analysis. The origin of the effect lies in the anomalously large shift of the Fermi level which at $T = 0$ is part way down a sudden

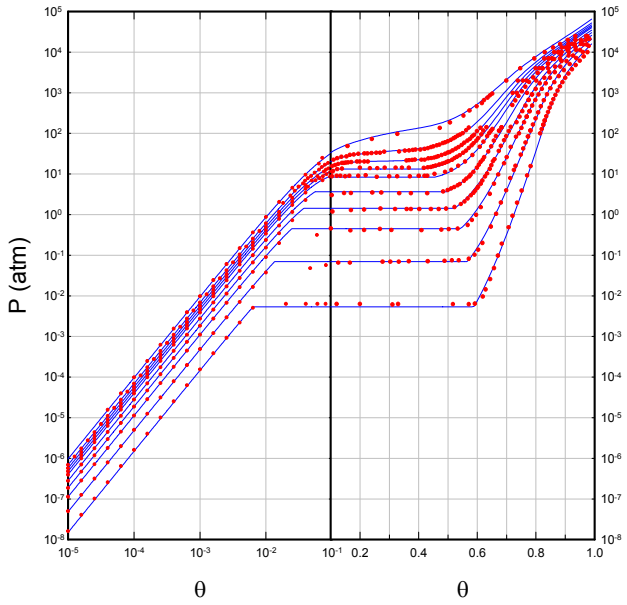

Figure 16. Isotherms and data points for the model with temperature-dependent fifth-order polynomial fit of $E_{\rm O}$ and optimized constrained fifth-order model for $\Delta E(\theta)$.

drop in the density of states (see Fig. 2 of Ref. [34]). We would not expect to see such a large shift due to the Fermi level at higher loading. This expectation is consistent with the rapid fall off of the spread with θ that can be seen in Fig. 15.

7.5. Phase diagram

The phase diagram that results from the lowest error constrained optimization is shown in Fig. 16. This phase diagram is very similar to the one we obtained with the unconstrained optimization. It looks very good in general.

8. Discussion and Conclusions

In this study we optimized a set of empirical models for the O-site energy, and in many cases also the O-site to T-site excitation energy, by minimizing the error between the model chemical potential and the isotherm data set. The general approach seems to be quite successful in giving models that match the isotherms of the data set, and also sheds light on the physical system. These are some of the simplest empirical models that can produce relatively high quality phase diagrams.

The optimization of a Lacher type of model with a temperature-independent O-site energy that is higher-order in θ is conceptually straightforward, and it produces better results than we had expected initially. We have not found such models studied systematically previously in the literature. The generalization to temperature-dependent O-site energies results in a phase diagram that is probably good enough to work with for some applications. The only problem

with it is that it does not correspond to a plausible physical model since the O-site energies decrease with temperature at low loading.

The issue of T-site occupation remains somewhat controversial at this time, primarily due to the lack of completely unambiguous experimental evidence showing explicitly significant T-site occupation. There is substantial theoretical support in density functional calculations and in quantum chemistry calculations for sufficiently low T-site energies such that one would expect them to have noticeable occupation and impact the phase diagram. The results from neutron diffraction experiments in palladium deuteride (showing T-site occupation) seem clear enough; however, the significance of these experimental results do not appear at this time to be widely appreciated. Consequently, our use of models with both O-site and T-site occupation in this work is likely to be acceptable to the theorists, and objectionable to the experimentalists.

Unconstrained optimization assuming both O-site and T-site occupation leads to models with very low mean square errors, but which are not physically acceptable at low loading since the O-site energy decreases with temperature. Constrained optimization with the excitation energy fixed at $\theta = 0$ fixes this problem, and results in a good match with low error. The biggest headaches in this case are that the excitation energy seems a bit low relative to the PdD neutron diffraction experiments, and the spread in the O-site energies in the mid-range of loading is larger than what we would hope for.

When we make use of a model with fixed $\Delta E(\theta)$ in Section 5, these problems are improved; the resulting phase diagram looks very good. In this case the only headache is that the error I is a bit larger, due mostly to the imposed boundary condition at $\theta = 1$. This draws attention to the extrapolation that we used for high loading, based on a generalization of the approach of Baranowski et al. [31]. The issue here is that in neither case does the extrapolation take into account possible T-site occupation. Additional experimental PCT data at high loading and at high temperature will be needed to resolve this issue.

In general these results strongly support the hypothesis that T-site occupation occurs and impacts the phase diagram. One could argue that the results are not site specific, as any other site with a similar excitation energy would work equally well. However, at this point for us there are no other obvious competitive candidates.

It seems useful to consider the arguments in support of T-site occupation briefly here. We have made use of a temperature-dependent O-site energy to account for configurational splitting that would be associated with a more general lattice gas model. The optimization of the associated parameters leads to models in the absence of T-site occupation with the wrong temperature dependence at low loading (as discussed in Section 4). Including T-site occupation corrects this, in the case that the O-site to T-site excitation energy is close to the empirical model discussed in Section 5. One interpretation is that this means that we would not expect a lattice gas model based on O-site occupation to give as good of a match to the data set as an equivalent lattice gas model which includes T-site occupation. In our earlier analysis of α-phase solubility, where the O-site to T-site excitation energy is lowest, and where we have access to a larger spread in temperature, the analysis is unambiguous [34]. With T-site occupation a good fit to the data can be obtained; without T-site occupation there is no hope for a physically acceptable model. Consequently, this earlier analysis weighs more heavily in support of T-site occupation, and the present study is supportive based on an analysis of different data over a larger range of loading. Our earlier analysis of PdH and PdD at high loading near room temperature also requires T-site occupation in order to make sense of published data. Here our basic conclusion is that the available PCT data for palladium hydride over the entire range of available temperature and loading independently provides support for T-site occupation.

The error I from the optimizations is the variance of the chemical potential. We can relate the associated standard deviation to the standard deviation of the fugacity approximately according to

$$\frac{\Delta\mu_{\rm H}}{k_{\rm B}T} = \frac{1}{2}\frac{\Delta f}{f}. \tag{33}$$

The lowest errors from the different models correspond to values of $\Delta\mu_{\rm H}$ near 3–4 meV. At low pressure the fugacity is very nearly equal to the pressure; at high pressure the fugacity can be much larger. In this case it may be that optimizations based on $\ln P$ instead of $\mu_{\rm H}$ would be preferred, as this would tend to reduce the weight associated with the (poorly known) high pressure points. This might be of interest in a future study.

Yet another issue that might be addressed in future work involves the issue of the statistical weight of the O-site states in the presence of splitting. Including temperature dependence of the O-site states as in the empirical models studied in this paper implies a splitting in the O-site states, where lower energy states have more occupation at low temperature, and with where higher energy states have more occupation at elevated temperature. In this kind of picture, we would expect a reduction in the associated entropy of the O-site states which would occur if the splitting were modeled explicitly. This has not been addressed in the models considered above. It may be possible to develop even better empirical models by including this effect.

We note that there are other approaches to modeling the phase diagram; for example, as in the recent analysis of Joubert and Thiébaut [5]. In this work the parameterization is a physical chemistry model in terms of the Gibbs energy rather than a physics type of parameterization in terms of site energies as we have used.

The optimizations reported here lead to estimates for the O-site and T-site energies, which are not so readily available otherwise from experiment. These energies are of interest as many groups at present work with density functional codes and quantum chemistry codes which predict them.

Appendix: No Abrupt Change Near a Loading of Unity

In the course of the review process the reviewer raised issues pointing out the absence of an abrupt change in the experimental data near a loading of unity, which underscores the absence of experimental support for T-site occupation at high loading.

In one communication the reviewer wrote:
The upper phase limit for the beta phase cannot be obtained simply by measuring the H/Pd (D/Pd) ratio because a second hydrogen-rich phase can form, thereby creating a two phase mixture beyond the limit of the beta phase that would have an overall composition above the fcc limit of the beta phase. This behavior is seen in the other hydride systems as well as in the behavior of fcc compounds containing C and N. Instead, the upper limit has to be based on seeing an abrupt change in slope of some measured value. In fact, this change in slope is detected in the data near D/Pd=0.98 using the resistivity and the temperature effect on the resistivity combined with the overall composition.

In another communication the reviewer wrote:
A phase boundary occurs at the composition at which another crystal structure forms with a greater concentration of the second atom. For example, the phase limit of beta-VH occurs at H/V=0.8 where another phase having the crystal composition of VH_2 forms (page 15, Fukai). If only the overall composition were measured, the composition would be seen to increase beyond 0.8. This increase alone would not reveal that the increase resulted from formation of the VH_2 phase rather than H being added to the beta phase. This limitation applies to PdH when the composition is noted to increase above H/Pd=1. In the absence of being able to detect the additional crystal structure, the boundary has to be identified by a change in behavior, such as a change in slope seen in the resistivity or chemical activity. Changes in slope of both are seen near D/Pd=1. Graphs showing the result of pressure reported by Baranowski et al. and the effect of temperature on the resistivity by Tripodi et al. are attached.

In other words, no evidence supports the ability of the beta phase to accommodate D or H above the normal filling of the O-sites. Extra D or H in the T-sites or in metal atom vacancies is not supported by the location of the upper phase boundary, at least to an amount of occupancy that the accuracy of the measurements permit.

A person might argue that even though no extra H were present, the H in the lattice might be distributed between the O and T sites while retaining a H/Pd ratio below unity at the upper boundary. Why this novel distribution might form would provide a challenge for the paper to explain.

These comments of the reviewer are interesting, and worth some additional discussion. The issues under discussion are relevant to the analysis presented in an earlier work [35], and somewhat less so to the analysis of this paper since we included phase diagram data only below $\theta = 1$.

When we began the earlier analysis we were expecting to see a sudden change in the chemical potential at the $\theta = 1$ boundary, consistent with intuition that suggested the O-site to T-site excitation energy is large near $\theta = 1$. A very large number of models were analyzed with an excitation energy between 350 meV and 600 meV, and the results showed an abrupt change where below $\theta = 1$ only O-site occupation occurred, and above $\theta = 1$ the O-sites were completely filled and only incremental T-site occupation occurred with increased loading. Predictions from these early models would correspond will to the expectation that one would expect a sharp boundary between the β-phase for $\theta < 1$ and a T-site phase for $\theta > 1$.

It took a long time to move past this initial perspective and investigate models with lower O-site to T-site excitation energies. Such models behave qualitatively differently in that there is no sharp boundary in the chemical potential, or in any readily observable model parameter, at $\theta = 1$. The 226 meV excitation energy estimated in [35] is sufficiently low that a smooth transition occurs with partial occupation of O-sites and T-sites below and above $\theta = 1$.

References

[1] F. Lewis, *The Palladium/Hydrogen System*, Academic Press, New York, 1967.

[2] E. Wicke, H. Brodowsky and H. Züchner, Hydrogen in palladium and palladium alloys, in *Hydrogen in Metals*, Vol. 2, Springer, Berlin, 1978, pp. 73–155.

[3] T.B. Flanagan and W.A. Oates, The palladium–hydrogen system, *Ann. Rev. Materials Sci.* **21** (1991) 269–304.

[4] F.D. Manchester, A. San-Martin and J.M. Pitre, The H–Pd (hydrogen–palladium) system, *J. Phase Equilibria* **15** (1994) 62–83.

[5] J.M. Joubert and S. Thiébaut, Thermodynamic assessment of the Pd–H–D–T system, *J. Nucl. Materials* **395** (2009) 79–88.

[6] Y. Ebisuzaki and M. O'Keeffe, The solubility of hydrogen in transition metals and alloys, *Prog. Solid State Chem.* **4** (1967) 187–211.

[7] W.M. Mueller, J.P. Blackledge and G.G. Libowitz, *Metal Hydrides*, Academic Press, New York, 1968.

[8] W. A. Oates and T.B. Flanagan, The solubility of hydrogen in transition metals and their alloys, *Prog. Solid State Chem.* **13** (1981) 193–272.

[9] T.B. Flanagan, Thermodynamics of Metal–Hydrogen Systems, in *Metal Hydrides*, Springer, New York, 1981, pp. 361–377.

[10] E. Wicke, Some Present and Future Aspects of Metal–Hydrogen Systems, *Zeitschrift für Physikalische Chemie* **143** (1985) 1–21.

[11] N.A. Gokcen, Interstitial Solutions, in *Statistical Thermodynamics of Alloys*, Springer, New York, 1986, pp. 149–193.

[12] L. Schlapbach, *Hydrogen in Intermetallic Compounds I,* Springer, New York, 1988.

[13] R. Lässer, Properties of Protium, Deuterium and Tritium in Selected Metals, in *Tritium and Helium-3 in Metals*, Springer, Berlin, 1989, pp. 48–107.

[14] Y. Fukai, *The Metal–Hydrogen System*, Springer, New York, 1991.

[15] M. Fleischmann, S. Pons and M. Hawkins, Electrochemically induced nuclear fusion of deuterium, *J. Electroanal. Chem. and Interfacial Electrochem.* **261**(1990) 301–308; Errata, **263** (1990) 187.

[16] M. Fleischmann, S. Pons, M.W. Anderson, L.J. Li and M. Hawkins, Calorimetry of the palladium–deuterium-heavy water system, *J. Electroanal. Chem. Interfacial Electrochem.* **287** (1990) 293–348.

[17] E. Storms, *The Science of Low Energy Nuclear Reactions: A Comprehensive Compilation of Evidence and Explanations about Cold Fusion*, World Scientific, Singapore, 2007.

[18] R.H. Fowler and C.J. Smithells, A theoretical formula for the solubility of hydrogen in metals, *Proc. Roy. Soc. London, Series A, Mathematical and Physical Sciences* **160** (1937) 37–47.

[19] J.R. Lacher, A theoretical formula for the solubility of hydrogen in palladium, *Proc. Roy. Soc. London, Series A, Mathematical and Physical Sciences* **161** (1937) 525–545.
[20] F.D. Manchester, Lattice gas aspects of metal–hydrogen system, *J. Less Common Metals* **49** (1976) 1–12.
[21] S. Dietrich and H. Wagner, Model calculation for the incoherent phase-transition in the palladium–hydrogen system, *Zeitschrift für Physik B Condensed Matter* **36** (1979) 121–126.
[22] C.K. Hall and M. Futran, Statistical theory of the phase change behavior of metal–hydrogen systems, *J. Less Common Metals* **74** (1980) 237–242.
[23] R.A. Bond and D.K. Ross, The use of Monte Carlo simulations in the study of a real lattice gas and its application to the alpha Pd–D system, *J. Phys. F: Metal Physics* **12** (1982) 597.
[24] C.K. Hall, A review of the statistical theory of the phase-change behavior of hydrogen in metals, *Electronic Structure and Properties of Hydrogen in Metals*, Springer, New York, 1983, pp. 11–24.
[25] E. Salomons, On the lattice gas description of hydrogen in palladium: a molecular dynamics study, *J. Physics: Condensed Matter* **2** (1990) 845.
[26] I.K. Robinson, Computational Studies of Hydrogen in Palladium, Doctoral dissertation, University of Salford, 2015.
[27] Y. Wang, S.M. Sun and M.Y. Chou, Total-energy study of hydrogen ordering in PdH_x $(0 \leq x \leq 1)$, *Phy. Rev. B* **53** (1996) 1.
[28] P.O. Orondo, A Theoretical Model of Interstitial Hydrogen: Pressure–Composition–Temperature, Chemical Potential, Enthalpy and Entropy, MIT PhD Thesis, 2012.
[29] J.E. Worsham, M.K. Wilkinson and C.G. Shull, Neutron-diffraction observations on the palladium–hydrogen and palladium–deuterium systems, *J. Phys. Chem. Solids* **3** (1957) 303–310.
[30] G. Nelin, A neutron diffraction study of palladium hydride, *Phys. Status Solidi (b)* **45** (1971) 527–536.
[31] B. Baranowski, S.M. Filipek, M. Szustakowski, J. Farny and W. Woryna, Search for "cold-fusion" in some Me–D systems at high pressures of gaseous deuterium, *J. Less Common Metals* **158** (1990) 347–357.
[32] I.F. Silvera and F. Moshary, Deuterated palladium at temperatures from 4.3 to 400 K and pressures to 105 kbar: search for cold fusion, *Phy. Rev. B* **42** (1990) 9143.
[33] M.C.H. McKubre, F.L. Tanzella and V. Violante, What is needed in LENR/FPE studies? *J. Cond. Mat. Nucl. Sci.* **8** (2012) 187.
[34] P.L. Hagelstein, O-site and T-site occupation of α-phase PdH_x and PdD_x, *J. Cond. Mat. Nucl. Sci.* **17** (2015) 67–90.
[35] P.L. Hagelstein, An empirical model for octahedral and tetrahedral occupation in PdH and in PdD at high loading, *J. Cond. Mat. Nucl. Sci.* **17** (2015) 35–66.
[36] J.D. Clewley, T. Curran, T.B. Flanagan and W.A. Oates, Thermodynamic properties of hydrogen and deuterium dissolved in palladium at low concentrations over a wide temperature range, *J. Chem. Soc., Faraday Trans. 1: Phy. Chem. in Condensed Phases* **69** (1973) 449–458.
[37] K.A. Moon, Pressure–composition–temperature relations in the palladium–hydrogen system, *J. Phy. Chem.* **60** (1956) 502–504.
[38] D.H. Everett and P. Nordon, Hysteresis in the palladium+hydrogen system, *Proc. Roy. Soc. London A: Mathematical, Physical and Engineering Sciences* **259** (1960) 341–360.
[39] J.W. Simons and T.B. Flanagan, Absorption isotherms of hydrogen in the α-phase of the hydrogen–palladium system, *J. Phy. Chem.* **69** (1965) 3773–3781.
[40] R. Burch, Theoretical aspects of the absorption of hydrogen by palladium and its alloys. Part 1. A reassessment and comparison of the various proton models, *Trans. Faraday Soc.* **66** (1970) 736–748.
[41] M.J.B. Evans and D.H. Everett, Thermodynamics of the solution of hydrogen and deuterium in palladium, *J. Less Common Metals* **49** (1976) 123–145.
[42] O.J. Kleppa and R.C. Phutela, A calorimetric-equilibrium study of dilute solutions of hydrogen and deuterium in palladium at 555 to 909 K, *J. Chem. Phys.* **76** (1982) 1106–1110.
[43] R. Lässer and G.L. Powell, Solubility of protium, deuterium and tritium in palladium–silver alloys at low hydrogen concentrations, *J. Less Common Metals* **130** (1986) 387–394.
[44] W.A. Oates, R. Lässer, T. Kuji and T.B. Flanagan, The effect of isotopic substitution on the thermodynamic properties of palladium–hydrogen alloys, *J. Phys. Chem. Solids* **47** (1986) 429–434.
[45] A. Harasima, T. Tanaka and K. Sakaoku, Cooperative Phenomena in Pd–H System I, *J. Phy. Soc. Japan* **3** (1948) 208–213.

[46] T. Tanaka, K. Sakaoku and A. Harasima, Cooperative Phenomena in Pd–H System II, *J. Phy. Soc. Japan* **3** (1948) 213–218.
[47] M.P. Pitt and E.M. Gray, Tetrahedral occupancy in the Pd–D system observed by in situ neutron powder diffraction, *Europhys. Lett.* **64** (2003) 344.